Journal of Hazardous Materials 177 (2010) 312–322

Contents lists available at ScienceDirect

Journal of Hazardous Materials

journal homepage: www.elsevier.com/locate/jhazmat

Biosorption of lead using immobilized *Aeromonas hydrophila* biomass in up flow column system: Factorial design for process optimization

S.H. Hasan [a,*], P. Srivastava [a], M. Talat [b]

[a] *Water Pollution Research Laboratory, Department of Applied Chemistry, Institute of Technology, Banaras Hindu University, Varanasi 221005, India*
[b] *Department of Biochemistry, Faculty of Science, Banaras Hindu University, Varanasi 221005, India*

ARTICLE INFO

Article history:
Received 11 June 2009
Received in revised form 7 December 2009
Accepted 7 December 2009
Available online 28 December 2009

Keywords:
Aeromonas hydrophila
Pb(II)
Bed Depth Service Time (BDST) Model
Central Composite Design (CCD)
Sorption–desorption

ABSTRACT

Free and immobilized biomass of *Aeromonas hydrophila* has been utilized for the removal of Pb(II) from aqueous solution. Fitness of Langmuir sorption model to the sorption data indicated the sorption was monolayer and uptake capacity of biomass was 163.9 and 138.88 mg/g for the free and immobilized biomass respectively. 85.38% Pb(II) removal was achieved at bed height of 19 cm and flow rate of 2 mL/min and BDST model was in a good agreement with the experimental results ($r^2 > 0.997$). An attempt has been made to optimize the process conditions for the maximum removal using Central Composite Design with the help of Minitab® 15 software and the result predicted by optimization plots was 88.27% which is close to the experimental data i.e. 85.38%. Sorption–desorption studies revealed that polysulfone immobilized biomass could reused up to 16 cycles and bed was completely exhaust after 33 cycles.

1. Introduction

Heavy metals have been a major cause of concern over the last few decades because of they are non-biodegradable and tend to accumulate in living organisms, thus becoming concentrated throughout the food chain [1]. Lead has been a major focus in wastewater treatment because it is associated with many health hazards [2]. The major bio-chemical effect of Pb(II) is its interference with heme synthesis, which leads to hematological damage. Lead is non-biodegradable cumulative toxin, which accumulates in the body and causes plumbism, increase in RBCs, interference with neuro-transmission, bone marrow damage, paralysis of wrist joints, degeneration of offspring, disturbance in cerebral function, kidney damage, etc. [3]. World Health Organization and United States Public Health Services have set a limit of 0.01 ppm as an acceptable limit of lead for drinking water. Thus, it is imperative that lead is removed from effluent before being discharged into the sewage system or into the aquatic environment.

There are several conventional techniques which are utilized for removing heavy metals from aqueous streams such as chemical precipitation as synthetic coagulants, solvent extraction, ion exchange and reverse osmosis [2]. The application of such traditional treatment techniques, however, needs enormous cost and continuous input of chemicals, which becomes impracticable and uneconomical and causes further environment damage [4,5]. Hence, the search for easy, effective, economical and eco-friendly technique is underway which is required for the fine tuning of effluent/wastewater treatment. Biosorption has been suggested as a potential alternative for detoxification and recovery of toxic and valuable metals from wastewater [6]. Batch experiments are generally done to measure the effectiveness of adsorption for removing specific adsorbates as well as to determine the maximum adsorption capacity. Different types of biomaterials viz. biomass of microorganisms and agricultural waste have been used for the removal lead using batch mode of sorption experiments [7–9]. However, from industrial point of view, the continuous adsorption in fixed bed column is often desired. It is simple to operate and can be scaled-up from a laboratory process. Few attempts have been made for the removal of lead from water using continuous mode [10–12]. The use of bacteria in this area of biosorption is advantageous [7]. However, the use of microbial biomass in its native form for large scale process utilization is not practicable because of its smaller particle size, poor mechanical strength and little rigidity. Other drawbacks include difficulty in the separation of biomass after biosorption, possible biomass swelling, inability to regenerate/reuse and development of high pressure drop in the column mode [13]. Immobilization of microbial biomass within polymeric matrix has been found to be practical for biosorption. It has several benefits including control of particle size, regeneration and reuse of the biomass, easy recovery of metal from the loaded beads using appropriate desorption techniques, thereby minimizing the possibilities of environmental contamination, high biomass loading

* Corresponding author. Tel.: +91 542 2575758.
E-mail address: hasanitbhu@yahoo.co.in (S.H. Hasan).

0304-3894/$ – see front matter © 2009 Elsevier B.V. All rights reserved.
doi:10.1016/j.jhazmat.2009.12.034

and minimal clogging under continuous-flow conditions [13,14]. The choice of immobilization matrix is a key factor in the environmental application of immobilized biomass. The polymeric matrix determines the mechanical strength and chemical resistance of the final biosorbent particles for successive biosorption cycles. Different techniques like flocculation, covalent bonding to carriers and encapsulation in polymer gel and entrapment in polymeric matrix are available for immobilization. The gel prepared from natural polysaccharides such as alginate, κ-carageenan is commonly used in cell immobilization [15]. These natural gels unfortunately abrade easily [16] or dissolve in the presence of competitive ions [17], thus limiting their application under actual effluent conditions. The use of polysulfone as a matrix or cell immobilization has been extensively studied in various biological systems [18,19]. Polysulfone offers various advantages over the conventional alginate hydrogels including high durability and chemical stability and is nontoxic to viable cells. Polysulfone is an amorphous, rigid, heat resistant and chemically stable thermoplastic material which has been identified as a good immobilizing agent [13,20]. In the present investigation, *Aeromonas hydrophila*, a gram-negative bacterium, was used in free and immobilized form to remove Pb(II) from aqueous solution in batch as well as continuous system. The effects of column parameters such as bed height and flow rate have been studied. Bed Depth Service Time (BDST) Model was applied on the experimental data. In addition to this, sorption–desorption experiments were also carried out for successive cycles. Furthermore, the effect of the variables i.e. flow rate and bed height, which are affecting the removal of Pb(II) in column system using immobilized biomass of *A. hydrophila*, were evaluated by using response surface methodology (RSM) (a statistical and graphical technique). Different factorial designs are available in RSM techniques [21,22]. Here, two-level two factor (2^2) full factorial Central Composite Design (CCD) model was used [23]. The predicted result by the response surface Central Composite Design (CCD) model was then compared with the experimental results.

2. Materials and methods

2.1. Preparation of standards and reagents

All chemicals and reagents used were of analytical grade and were used without further purification (purchased from E. Merck, India Ltd., Mumbai, India). Stock solutions of 1000 mg/L Pb(II) were prepared from $Pb(NO_3)_2$ in de-ionized, double distilled water containing a few drops of concentrated HNO_3 to prevent the precipitation of Pb(II) by hydrolysis. Required initial concentration of Pb(II) samples was prepared by appropriate dilution of the above stock Pb(II) standard solution. Standards for calibration of AAS for Pb(II) were prepared from standard solution of lead purchased from Merck, Germany.

2.2. Preparation of biosorbent

The strain used in this study was *A. hydrophila* (MTCC 646)-a pure culture-obtained from the Microbial Type Culture Collection & Gene Bank, Institute of Microbial Technology, Chandigarh, India. The culture was routinely maintained at 4 °C on nutrient agar medium slant and aerobically cultivated in nutrient broth containing beef extract 10 g/L, NaCl 5 g/L and peptone 20 g/L. The initial pH of the culture was adjusted from 7.0 to 7.5. The flasks were incubated at 30 °C in an electrically thermostated rotatory shaker agitated at 200 rpm for 24 h. The growing cells from the culture broth were separated from the liquid by centrifugation at 5000 rpm for 5 min and were washed with de-ionized water. The wet cell biomass was dried for 24 h at 60 °C in an oven. Dried cells were powdered by a blender in uniform size (100 μm) and were used for experiment (50 mL of bacterial cell suspension containing 3.2 g of biomass on a dry weight basis).

Table 1
Characterization and composition of dried biomass *Aeromonas hydrophila*.

Properties	*Aeromonas hydrophila*
Characterization	
Surface area (m^2/g)	0.676
Single point surface area at $P/P_o = 0.321904273$:	
BET surface area	0.689
Pore volume (cm^3/g)	0.849
Single point adsorption total pores less than 1506.8.500 Å at $P/P_o = 0.986989152$	
Pore size (Å)	53688.860
Adsorption average pore width (4V/A by BET):	
Particle density (g/cm^3)	0.320
Bulk density (g/cm^3)	0.119
Porosity	0.629
Particle size (μm)	100
Relative humidity	1.200
pH_{ZPC}	3.5
Composition	
Carbon	25.790%
Nitrogen	7.230%
Sulfur	1.260%

2.3. Characterization and composition of the dried biomass of A. hydrophila

The surface area of the biomass was determined by a Micromeritics surface area analyzer (Model ASAP 2020, USA). Particle density was determined with the help of specific gravity bottles methods based on the Archimedes' principle. Bulk density of biomass was measured with Archimedean immersion methods. Particle size was analyzed by sieve analysis with the help of 150 No. BSS sieve. Humidity of biomass was analyzed by psychrometer (DTH 31 digital psychrometer). The points of zero charge (pH_{ZPC}) of the dead biomass of *A. hydrophila* were determined by the solid addition method [24,25]. All the results are reported in Table 1. For the composition, biosorbent was subjected to elemental analysis (Carbon, nitrogen and sulfur) and given in Table 1 [26].

2.4. Immobilization in polysulfone

100 mL of N,N-dimethylformamide (DMF) solution was added into a mixture consisting of 7 g of powdered biomass and 10 g of polysulfone (Himedia Chemical). After continuous stirring of mixture on magnetic shaker, uniform slurry of biomass was formed. The slurry was then added in a drop-wise manner (using a syringe (5 mL)) to a glass beaker containing distilled water. Beads were cured by stirring in distilled water for 8 h. After curing, the beads were air dried at room temperature for 2–3 days. Blank polysulfone beads were also prepared without adding the biosorbent.

2.5. Batch sorption experiments

Biosorption experiments were performed in 250 mL conical flasks previously rinsed with HNO_3 in order to remove any metal that remained unabsorbed on the glass wall. The pH of the metal solutions in the conical flask was initially adjusted to desired values by using 0.1 M/HNO_3/NaOH; the sorbents (free biomass and immo-

bilized biomass) were added to each flask and were agitated on the shaker until the equilibrium was reached. The sorbent (free biomass and immobilized biomass), separated by centrifugation/filtration at 15,000 rpm for 5 min, was analyzed for remaining Pb(II) concentration in the sample. The biosorption capacity of the metal ion was calculated by the equation:

$$q = \frac{(C_o - C_e)V}{M} \quad (1)$$

where q (mg/g) is the metal uptake, V (mL) is the volume, M (mg) is the amount of biomass and C_o (mg/L) and C_e (mg/L) are the initial and equilibrium metal concentrations respectively. All experiments in this work were conducted in triplicate.

2.6. Column design and experimental procedure

Experiments were carried out in glass column of 30 cm height and 2.0 cm internal diameter, filled with different quantities of immobilized biomass. In the column, 0.5 mm stainless steel mesh and 1.0 cm glass wool were kept at the bottom and at the top of the column respectively to support the immobilized *A. hydrophila* beads in the column and to ensure a closely packed arrangement. A 3.0 cm layer of glass beads was placed at the column base for providing a uniform inlet flow and good Pb(II) solution distribution into the column. The Pb(II) solution was pumped through peristaltic pump (Miclins India, Model No. PP 20) connected at the bottom of the column in an upward direction (Graph not given). The treated Pb(II) solution was collected from the top with same flow rate of feed stream and was estimated for the Pb(II) concentration. Operation of the column was stopped when effluent metal concentration exceeded a value of 98% of the initial metal ion concentration. Desorption was carried out by passing 0.01 M HCl through the column bed in upward direction at a flow rate of 4.0 mL/min. The effluent metal solution was collected and analyzed for Pb(II) content. On the completion of desorption cycle, the column was rinsed with de-ionized double distilled water in the same manner as for biosorption till the eluting distilled water attains pH 7.0. The desorbed and regenerated column bed was reused for next cycle. Another cycle of sorption–desorption was repeated in the same manner as above mentioned. All the experiments were performed in triplicates at 30 °C temperature, 5.0 pH and atmospheric pressure (760 mm).

2.7. Analysis of Pb(II) in aqueous solution

A Shimadzu AA-6300 (Japan) atomic absorption spectrophotometer was used as detector with hollow cathode lamp light source set at 283.3 nm wavelength using 10 mA lamp current and 0.7 nm slit width, and with deuterium lamp for background correction. Instrument grade (98%) acetylene, delivered at 4.0 L/min at a pressure of 0.9 kg/cm^2 was used to generate the flame for the AAS together with compressed air supplied at 17.5 L/min flow rate and 3.5 kg/cm^2 gas pressure. The instrument was calibrated from 0.1 to 10.0 mg/L. Other range samples were diluted until results within the calibration range were obtained.

2.8. Modeling and analysis of column data

To analyze the dynamic Pb(II) removal in up flow fixed bed column, breakthrough curves (C_t/C_0 vs. time) were drawn and the data were evaluated with the help of following equations as previously used by [27]:

Effluent volume:

$$V_{eff} = F \cdot t_e \quad (2)$$

Total amount of Pb(II) sent to column:

$$M_{total} = \frac{C_o F t_e}{1000} \quad (3)$$

Total percentage removal of Pb(II):

$$\text{Total Pb(II) removal (\%)} = \frac{m_{ad}}{M_{total}} \times 100 \quad (4)$$

Length of the mass transfer zone:

$$Z_m = Z\left(1 - \frac{t_b}{t_e}\right) \quad (5)$$

The Pb(II) desorbed (m_d) can be calculated from the area below the desorption curve (outlet Pb(II) concentration vs. time) multiplied by the flow rate. The desorption efficiency can be calculated from

$$\text{Desorption efficiency (\%)} = \frac{m_d}{m_{ad}} \times 100 \quad (6)$$

where t_b is the breakthrough time at which the outlet Pb(II) concentration reached 1 mg/L, t_e is the exhaustion time at which the outlet Pb(II) concentration exceeded 95% of that at the inlet concentration. The total quantity of Pb(II) biosorbed in the column (m_{ad}) was calculated from the area above the breakthrough curve (outlet metal concentration vs. time) multiplied by the flow rate (F). Dividing m_{ad} by the biosorbent mass (M) leads to the uptake capacity (Q) of the biomass.

In the fixed bed systems, the main design criterion is to predict how long the adsorbent material will be able to sustain removing a specified amount of impurity from solution before regeneration is needed. This period of time is called the service time of the bed. Hutchins [28] proposed a simple approach to fixed bed adsorbers to correlate the service time with the process variables:

$$t = \frac{N_o Z}{C_o u} - \frac{1}{k_a C_o} \ln\left(\frac{C_o}{C_t} - 1\right) \quad (7)$$

The model is termed as the Bed Depth Service Time (BDST) model. Here t is the service time, N_o is the dynamic bed capacity (mg/L), Z is the bed height of the column (cm), u is the influent linear velocity (cm/min) defined as the ratio of the volumetric flow rate F (mL/min) to the cross sectional area of the bed S_c (cm^2), C_t is the effluent concentration of solute in the liquid phase (mg/L), C_o the initial concentration of solute in the liquid phase (mg/L) and k_a is the rate constant in BDST model (L/mg h).

2.9. Response surface methodology

RSM is a combination of mathematical and statistical techniques used for developing, improving and optimizing the processes and used to evaluate the relative significance of several affecting factors even in the presence of complex interactions. RSM usually contain three steps: (1) design and experiments; (2) response surface modeling through regression; (3) optimization. The main objective of RSM is to determine the optimum operational conditions of the process or to determine a region that satisfies the operating specifications. The application of statistical experimental design techniques in adsorption process development can result in improved product yields, reduced process variability, closer confirmation of the output response to nominal and target requirements, and reduced development time and overall costs [29,30]. Varieties of factorial designs are available to accomplish this task. The most successful and best among them is the Central Composite Design (CCD). It is obtained by adding two experimental points along each coordinate axis at opposite sides of the origin and at a distance equal to the semi-diagonal of the hyper cube of the factorial design. The

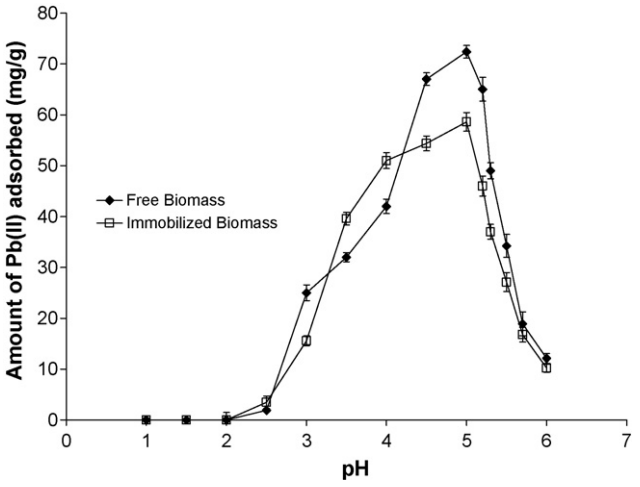

Fig. 1. Effect of pH: initial Pb(II) concentration = 103.6 mg/L, 30 °C temperature. Vertical bars show the standard deviation of three replicates.

new extreme values (low and high) for each factor are added in this design [31]. If the factorial is a full factorial, then

$$\alpha = [2^k]^{1/4} \tag{8}$$

Since in this study two factors such as flow rate and bed height of Pb(II) removal were considered thus $k = 2$. So $\alpha = 1.414$.

Furthermore, the total number of experiments points (N) in a CCD can be calculated from the following equation:

$$N = 2^k + 2k + X_o \tag{9}$$

where N is the total number of experiments, k is the number of variables and X_o is the number of central points. Thus, for this design, total number of experimental runs will be 13 ($k = 2$; $X_o = 5$) and one alpha value.

Data from the Central Composite Design were subjected to a second-order multiple regression analysis to explain the behavior of the system using the least squares regression methodology for obtaining the parameter estimators of the mathematical model [31]:

$$Y = \beta_0 + \Sigma\beta_i X_i + \Sigma\beta_{ii} X_i^2 + \Sigma\beta_{ij} X_i X_j + \varepsilon \tag{10}$$

where Y is the response, β_0 is the constant, β_i is the slope or linear effect of the input factor X_i, β_{ii} is the quadratic effect of input factor X_i, β_{ij} is the linear by linear interaction effect between the input factor X_i and ε is the residual term.

MINITAB® Release 15, developed by Minitab Inc., USA, a statistical software package [32], was used for regression analysis of the data obtained and to estimate the coefficient of regression equation. Analysis of variance (ANOVA), which is a statistical testing of the model in the form of linear terms, squared terms and the interaction, was also utilized to test the significance of each term in the equation and the goodness of fit of the regression model obtained. This Response Surface Model was also used to predict the result by contour plots in order to study the individual and cumulative effects of the variables and the mutual interactions between the variables on the dependent variable. Optimization curves were plotted in order to confirm the experimental results and to achieve the required removal of lead by choosing the predicted conditions.

3. Results and discussion

3.1. Effect of pH

Fig. 1 shows the biosorption of Pb(II) by free biomass and polysulfone immobilized biomass as a function of pH (preliminary tests confirmed that the blank polysulfone beads exhibited negligible lead uptake (data not shown)). The uptake capacities of the two sorbents generally showed a similar trend: an increase in uptake with pH increase at lower pH range (pH 2.0–5.0), with effect leveling off beyond pH 5.0. It was also noted that the polysulfone immobilized biomass has a much lower uptake capacity than the free biomass at the same pH. The effect of pH on the capacity for Pb(II) biosorption by *A. hydrophila* was studied and the optimum biosorption capacity was obtained at pH 5.0 for both free and polysulfone immobilized biomass. It was observed that the Pb(II) biosorption was relatively less at low pH values (pH 2–3). The less metal uptake at these pH conditions may be explained on the basis of binding sites being protonated, resulting in a competition between H^+ and Pb(II) ions for occupancy of binding sites [33]. As the pH increased and surface functional groups got activated, it resulted in increased Pb(II) sorption and the sharpest increase in Pb(II) uptake was observed in the pH range of 3–5. Further increase in pH resulted in decline in Pb(II) uptake in both the cases. When pH is higher than 5, the precipitation of insoluble metal hydroxides takes place thus lower the biosorption efficiency [2]. In addition to this at the equilibrium condition, the optimum and initial pH 5.0 of the metal solution slightly increased i.e. 5.32 and 5.15 for free and immobilized biomass respectively. This could have resulted due to dissolution of certain minerals, such as, carbonates from the biomass [34,35]. This process became rapid with increase of initial pH from 5.2 to 6.0 and thus uptake capacity was decreased. So for further investigation, an optimized pH of 5.0 is taken for all the biosorption experiments for both free and immobilized biomass respectively.

3.2. Isotherm studies

The Langmuir isotherm model [36], valid for monolayer sorption onto a surface of a finite number of identical sites, is given by Eq. (11):

$$\frac{C_e}{q_e} = \frac{1}{Q^\circ b} + \frac{C_e}{Q^\circ} \tag{11}$$

where Q^o is the maximum metal uptake (mg/g) and b is the Langmuir affinity constant (L/mg). The constant b represents the affinity between the sorbent and the sorbate. The plot of C_e vs. C_e/q_e (Fig. 2) of the Langmuir isotherm was found to be linear and the maximum Pb(II) uptake (Q^o) was observed as 163.93 and 138.88 mg/g for free and immobilized biomass respectively at pH 5.0, 30 °C temperature and 51.8–259 mg/L of Pb(II) concentration range. The constant b was recorded as 0.025 and 0.033. The correlation coefficients were 0.997 and 0.993 for free and immobilized biomass respectively. The Langmuir uptake capacity (Q^o) of free biomass was greater than that of the polysulfone immobilized biomass. This variation could be due to many reasons. First, the binding of cationic and anionic metal species to the bacterial cell wall is assumed to occur predominantly through surface adsorption. Second, the mass transfer of the metal ions from aqueous phase to the solid sorbent sites is dependent on porosity of the sorbent. Third, the native biomass in contact with the metal ions under the conditions of moderate agitation has its binding sites freely exposed to the sorbate. However, in immobilized systems, the sorbent particles entrapped and retained at the interior may not have accessibility to the metal ions [37].

Table 2
Column data for packed bed immobilized beads column for biosorption of Pb(II) onto immobilized *A. hydrophila* at different bed height (cm) and flow rate (mL/min).

C_o (mg/L)	Flow rate (mL/min)	Bed height (cm)	Uptake (mg/g)	t_b (h)	t_e (h)	V_{eff} (mL)	%Metal removal
103.6	2.0	7	36.68	18.53	27.91	3349.2	51.18
103.6	2.0	10	42.90	25.53	37.17	4460.4	65.00
103.6	2.0	13	43.80	37.42	59.13	7095.6	76.81
103.6	2.0	16	46.52	40.42	62.50	7500.0	79.25
103.6	2.0	19	54.50	44.87	68.29	8184.0	85.38
103.6	4.0	19	53.32	24.9	36.00	8640.0	79.23
103.6	6.0	19	52.42	16.0	24.50	8820.0	76.31
103.6	8.0	19	49.89	12.5	19.00	9120.0	70.23
103.6	10.0	19	49.34	9.54	15.50	9300.0	68.12

C_o, Initial Pb(II) concentration; t_e, exhaustion time (h); t_b, breakthrough time (h); V_{eff}, volume effluent (mL).

3.3. Effect of bed height and flow rate

In order to optimize bed height for maximum Pb(II) removal, experiments were carried out by varying the bed height 7.0, 10.0, 13.0, 16.0 and 19.0 cm by the addition of 4.9, 7.0, 9.1, 11.2, and 13.3 g of polysulfone immobilized biomass into the column at flow rate of 2.0 mL/min and 103.6 mg/L Pb(II) concentration. The plot of effluent Pb(II) concentration vs. time (C_t/C_o vs. time) at different bed heights is shown in Fig. 3. The breakthrough time, exhaustion times, percentage Pb(II) removal and uptake capacity were calculated from the breakthrough curves and are presented in Table 2. Result indicates that the breakthrough time, exhaustion time, uptake capacity, percentage removal and volume treated increased with the rise in bed height from 7.0 to 19.0 cm. This displacement of the front of adsorption with the increase in bed depth can be explained by mass transfer phenomenon that takes place in this process. When the bed depth is reduced, axial dispersion phenomenon predominates in the mass transfer and reduces the diffusion of metallic ions. The solute (metallic ions) has not enough time to diffuse into the whole adsorbent mass. Consequently, an important reduction in the volume treated at breakthrough point was observed. Moreover, an increase in the bed adsorption capacity was noticed at the breakthrough point with the increase in the bed height. This increase in adsorption capacity with increase in the bed height can be due to the increase in the specific surface of the adsorbent, which supplies more fixation binding sites. It follows that a delayed breakthrough of the Pb(II) leads to an increase in the volume of the solution treated. The increase in adsorption with increase in bed depth was due to an increase in the adsorbent doses in larger bed, which provides greater service area (or adsorption sites) [13,38,39].

The effect of flow rate on Pb(II) sorption was studied by varying the flow rate (2.0. 4.0, 6.0, 8.0 and 10.0 mL/min) at bed height of 19 cm and 103.6 mg/L of initial Pb(II) concentration. The plot of C_t/C_0 vs. time at different flow rate is also shown in Fig. 3. The total sorbed Pb(II) ion, breakthrough time, exhaustion time, percentage Pb(II) removal and uptake capacity decreases with increase of flow rate from 2.0 to 10.0 mL/min except treated volume effluent which increases with flow rate as presented in Table 2. Results indicate that percentage removal of metal ion reduces as the flow rate increases. An increase in the flow rate decreases the service time of the bed. This is due to the decrease in contact time between the metal ions and the immobilized biomass at higher flow rates. As the adsorption rate was controlled by intra particulate diffusion, an early breakthrough occurring leading to low percentage removal. These results were also in agreement with those referred to the literature [40,41]. When the flow rate decreases, the contact time in the column is longer as intra particulate diffusion then becomes effective. Thus, the Pb(II) has more time to diffuse onto the immobilized biomass and better percentage removal is obtained. At a higher flow rate, the biosorbent gets saturated early (certainly because of reduced contact time); a larger amount of ions is adsorbed onto the immobilized biomass and a weak distribution of the liquid is there into the column. This leads to a lower diffusivity of the solute onto the immobilized biomass.

3.4. Bed Depth Service Time (BDST) model

The BDST plot of service time (t_b) against bed height (Z) at different flow rates (2–10 mL/min) was found to be linear with high

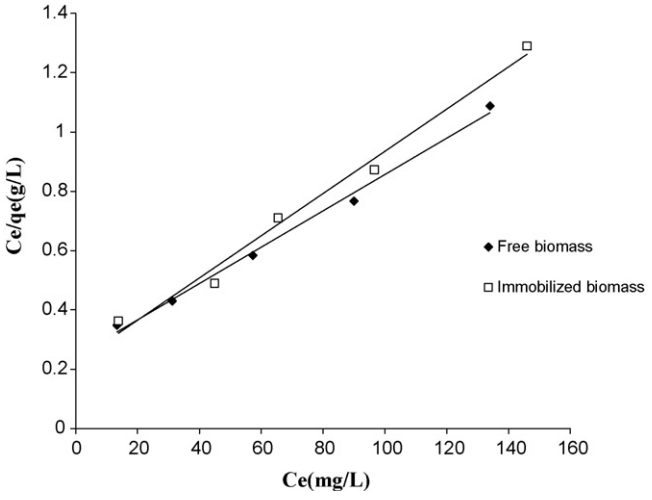

Fig. 2. Langmuir isotherm plot (pH = 5.0, temperature = 30 °C, Initial Pb(II) concentration range = 51.8–259 mg/L).

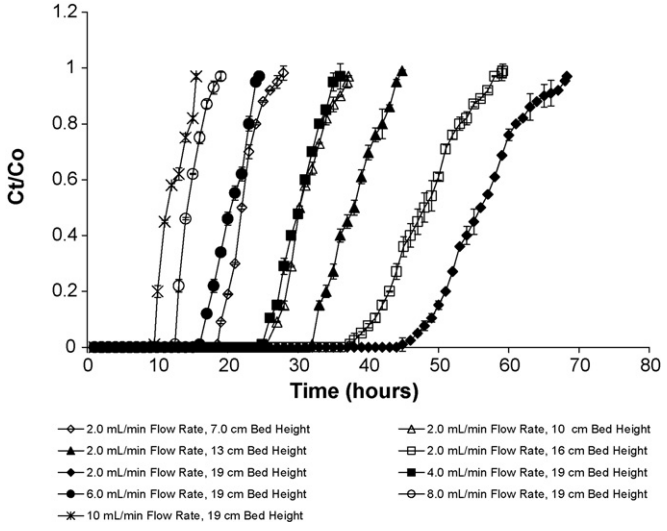

Fig. 3. Breakthrough curve for Pb(II) sorption at different bed heights and flow rate: pH = 5.0, temperature = 30 °C, initial Pb(II) concentration = 103.6 mg/L. Vertical bars shows the standard deviation of three replicates.

Table 3
Bed Depth Service Time model parameters for sorption of Pb(II) onto immobilized *A. hydrophila*.

Flow rate (mL/min)	Inlet metal concentration (mg/L)	N_o (mg/L)	k_a (L/mg h)	r^2
2.0	103.6	148.623	0.0109	0.998
4.0	103.6	151.689	0.0270	0.998
6.0	103.6	152.430	0.0277	0.998
8.0	103.6	182.916	0.0626	0.997
10.0	103.6	183.444	0.0558	0.996

N_o, bed capacity (mg/L) and k_a, rate constant (L/mg h).

correlation coefficient (0.997) indicating the validity of the BDST model for the present system (Graph not given). With the help of this plot (BDST), the bed sorption capacity (N_o) and sorption rate constant (k_a) were calculated from the slope and intercept as given in Table 3. It has been found that the rate constant (k_a) and the bed sorption capacity (N_o) increased from 0.0121 to 0.0558 L/mg h and 142.024–183.444 mg respectively with increase of flow rate from 2 to 10 mL/min. If k_a is large, even a short bed will avoid breakthrough, but as k_a decreases a progressively longer bed is required to avoid breakthrough. The values of constants obtained from the BDST plot can be extrapolated for alternative flow rates by modifying the equation. A simplified form of this model is: $t = aZ - b$, where a is the slope, $a = \frac{N_o Z}{C_o u}$ and b is the intercept, $b = \frac{1}{k_a C_o} \ln\left(\frac{C_o}{C_r} - 1\right)$. When a new flow rate, other than the one used in the development of constants, is used to the column system, the equation can be modified by utilizing the new slope and intercept, $a' = a\ u/u' = F/F'$ where a and u are the old slope and influent linear velocity respectively and a' and u' are the new slope and influent linear velocity. As the column used in experiment has the same diameter, the ratio of original (u) and the new influent linear velocity (u') and original flow rate (F) and new flow rate (F') will be equal. The use of BDST model in this way provides a realistic description of the adsorption of Pb(II) by *A. hydrophila* biomass and the empirical data can be adopted for predicting the bed depth or service time for a specified set of influent characteristics for the scale-up of the sorption column.

3.5. Sorption–desorption studies

A successful biosorption process operation required the multiple reuses of the sorbent, which greatly reduced the process cost as well as decreased the dependency of the process on continuous supply of the sorbent. The sorption performance of immobilized biomass of *A. hydrophila* was evaluated in three sorption–desorption cycles. The breakthrough time (t_b), exhaustion time (t_e), Pb(II) uptake, % removal and critical bed length (Z_m) for all the three sorption cycles were calculated and are presented in Table 4. It can be seen from Fig. 4(a) that with the progress of sorption cycle, the breakthrough curve became flat as a result of the decrease of breakthrough time and increase in exhaustion time. The overall performance of the biosorbent in all the three cycles was very satisfactory as both very high Pb(II) uptake (54.50 mg/g) and % removal efficiency (85.38%) were observed. The minimum bed length (Z_m) required to obtain the breakthrough at $t = 0$ (also called critical bed length = critical bed length is the length of mass transfer zone and calculated through Eq. (5)) uniformly increased with progressive cycles, indicating the broadened mass transfer zone. Since a uniform decrease in sorption performance was observed with progressive cycles, the life of the biosorbent can be predicted based on the important column parameters.

For this purpose, three parameters were taken into consideration: breakthrough time, column uptake and critical bed length.

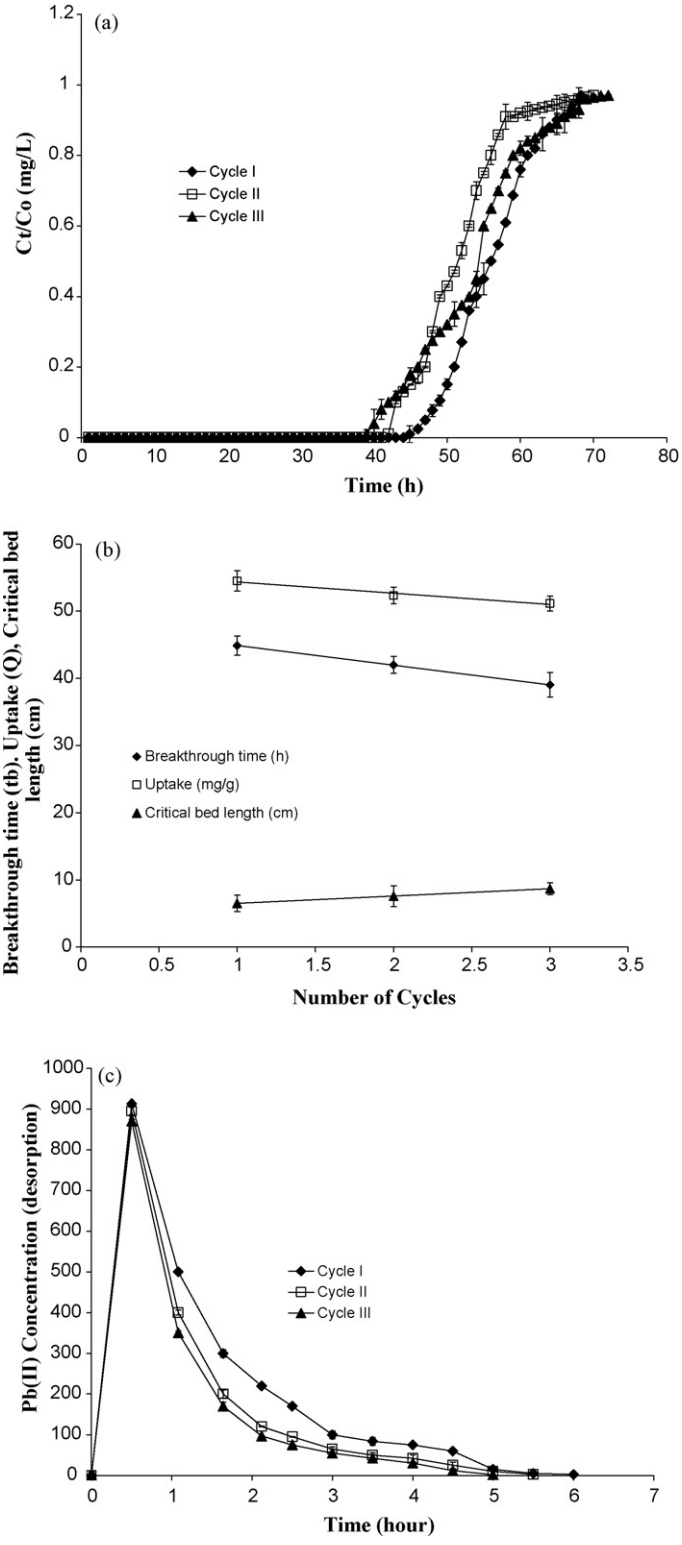

Fig. 4. (a) Sorption breakthrough curve during three sorption cycle (flow rate = 2.0 mL/min, pH = 5.0, temperature = 30 °C, initial Pb(II) concentration = 103.6 mg/L, Bed height = 19 cm). Vertical bars show the standard deviation of three replicates. (b) Linear plots of breakthrough time and Pb(II) uptake and critical bed length with respect to the number of cycles. Vertical bars show the standard deviation of three replicates. (c) Column desorption curve during three desorption cycle (desorbing agent 0.01 HCl, Flow rate = 4.0 mL/min. Vertical bars show the standard deviation of three replicates).

Table 4
Sorption–desorption process parameter for three sorption–desorption cycles.

Cycle no.	C_o mg/L	Z (cm)	Z_m (cm)	Uptake (mg/g)	t_b (h)	t_e (h)	V_{eff} (mL)	% Pb(II) removal	Desorption time(h)	%Desorption efficiency
1	103.6	19	6.52	54.50	44.87	68.29	8184.0	85.38	6.0	95.6
2	103.6	19	7.6	52.34	42	70.00	7740.0	80.0	5.5	95.0
3	103.6	19	8.72	51.14	39	72.00	7440.0	76.0	5.0	92.0

Z, bed height (cm); Z_m, bed length (cm); t_e, exhaustion time (h); t_b, breakthrough time (h); V_{eff}, Volume effluent (mL).

Table 5a
Number of experimental runs required and their details for two-level two factors full Factorial CCD Design.

Factors	Replicates	Central Composite Design		Total blocks	Total runs
		Base runs	Base blocks		
2	1	13	1	1	13
2 level two factors: full factorial CCD					
Cube points		Center points in cube	Axial points	Center points in axial	α
4		5	4	0	1.41421

The following forms of linear regression can be used [13,27,42]:

$$t_b = t_b i + kt_b n \quad (12)$$

$$Q = Q_i + kQ_n \quad (13)$$

$$Z_m = Z_{mi} + kZ_{mn} \quad (14)$$

where $t_b i$, Q_i and Z_{mi} are the initial breakthrough time, column uptake and critical bed length respectively; kt_b, kQ and kZ_m represent life factors corresponding to the breakthrough time, uptake and critical bed length respectively and n represents the cycle number. From the plot of t_b vs. n (Fig. 4(b)), $t_b i$ and kt_b were found to be 47.82 and 2.935 h/cycle respectively. Thus, the biosorbent bed can be predicted to have sufficient capacity to avoid the breakthrough at time $t = 0$ for up to 16 cycles. From the plot of Q vs. n (Fig. 4(b)), the expression $Q = 56.02 - 1.68n$ was also formulated. From this expression, it can be estimated that the bed would be completely exhausted (zero uptake) after 33.34 cycles. A value of 5.4 cm was determined for Z_{mi}, giving $kZ_m = 1.1$ cm/cycle (Fig. 4(b)) implying that breakthrough would appear at time $t = 0$ after 4.9 cycles. The correlation coefficients for all the three plots were 0.999, 0.986, and 0.995. Thus, it can be generalized that the sorption zone would reach the top of the bed after 16 cycles and column bed would be completely exhausted after 33.34 cycles.

Desorption curves observed in all the cycles exhibited a similar trend; a sharp increase at the beginning followed by a gradual decrease (Fig. 4(c)). The flow rate was maintained at 4.0 mL/min to avoid over contact of the desorbent with the biosorbent. The desorbent performed very well (0.1 M HCl) exhibiting desorption efficiencies greater than 92% (Table 4). The desorption process was carried out for an average of 5.5 h, compared to 64.93 h for the sorption process, and resulted in highly concentrated Pb(II) solutions in only a small volume of desorbent. For instance, in cycle 1 at $t = 0.5$ h, the effluent Pb(II) concentration was 913.130 mg/L.

3.6. Central Composite Design (response surface methodology approach)

A 2^2 full factorial Central Composite Design (CCD) of response surface methodology was applied to predict the effect of flow rate (mL/min; X_1) and bed height (cm; X_2) on the removal of Pb(II) in column system using MINITAB® 15 (Trial version) software [32]. The parameters were coded at five levels: $-\alpha$, -1, 0, 1 and α. For flow rate, the different levels studied are 2, 4, 6, 8 and 10 mL/min and for bed heights, the levels are 7, 10, 13, 16 and 19 cm. Since, in the present investigation, there are two variables, 14 experimental runs were required as per 2^2 full factorial designs (Table 5a). Experiments were performed according to the above experimental plan and the results are given in Table 5b along with the results predicted by the model with the help of software's. Significant changes in removal of lead were observed for all the combinations implying that all the variables were significantly affecting the sorption of lead.

3.6.1. Interpretation of the regression analysis

Multiple regression analysis was carried out to analyze the sorption data through Student's T-test and Probability P-values. The T-value is used to determine the significance of the regression coefficients of the parameters, and the P-value is defined as the smallest

Table 5b
Full factorial Central Composite Design Matrix of two factors along with experimental and predicted % removal of Pb(II).

Std. Order	Run Order	Pt Type	Blocks	Flow rate X_1 (mL/min)	Bed height X_2 (cm)	Experimental. % Removal	Predicted % Removal	Residual
10	1	−1	2	8	10	50.90	50.5800	0.3200
14	2	0	2	6	13	63.18	62.7600	0.4200
13	3	0	2	8	16	63.87	64.9760	−1.1060
8	4	−1	2	4	10	58.93	60.2996	−1.3696
12	5	0	2	6	13	63.18	62.7674	0.4126
11	6	−1	2	4	16	72.51	75.2963	−2.7863
9	7	−1	2	6	13	63.18	62.7674	0.4126
3	8	1	1	6	13	63.18	62.7674	0.4126
7	9	0	1	6	19	76.31	74.9827	1.3273
5	10	0	1	2	13	76.81	75.3510	1.4590
4	11	1	1	6	13	63.18	62.7674	0.4126
6	12	0	1	6	13	63.18	62.7674	0.4126
1	13	1	1	10	13	55.10	55.3210	−0.2210
2	14	1	1	6	7	45.51	45.5994	−0.0894

Table 6a
Estimated regression coefficients for the Pb(II) removal onto immobilized biomass of *A. hydrophila*.

Term	Coefficient	Standard error coefficient	*T*-value	*P*-value
Constant	62.7674	0.5411	115.998	0.000
X_1	−10.0150	0.8147	−12.293	0.000
X_2	14.6917	0.8147	18.034	0.000
$X_1 \times X_1$	2.5687	1.1479	2.238	0.056
$X_2 \times X_2$	−2.4763	1.1479	−2.157	0.063
$X_1 \times X_2$	−0.6100	2.8221	−0.216	0.834

$S = 1.411$, $R^2 = 98.39\%$, R^2 (pred) = 86.62%, R^2 (adj) = 97.39%.

level of significance leading to rejection of null hypothesis. In general, the larger the magnitude of *T* and the smaller the value of *P*, the more significant is the corresponding coefficient term [30]. The constant, which does not depend on any variable and interaction of variables, shows that the average percentage removal of Pb(II) on *A. hydrophila* was 62.7674 and that this average percentage removal is independent of the factors set in the experiment (Table 6a). The effect of the linear factors, i.e. flow rate and bed height were found to be highly significant ($P = 0.000$) on the removal of Pb(II), i.e. there is a linear relation of all these parameters with the percentage removal of Pb(II). All the quadratic terms were not found to be significant ($P > 0.05$). Quadratic terms are used to evaluate whether or not there is curvature (quadratic) in the response surface [31]. The interaction terms of flow rate and bed height ($P = 0.834$) were not found to be significant. A positive sign of the coefficient represents a synergistic effect, while a negative sign indicates an antagonistic effect. The linear term flow rate (−10.0150) and quadratic term bed height (−2.4763) and the interaction term flow rate and bed height have a negative (−0.6100) relationship with the biosorption process. The effect of linear term bed height (+14.6917) and quadratic term flow rate (+2.5687) has a positive effect on the removal of Pb(II) i.e., with an increase in bed height and flow rate, there will be an increase in the percent removal of Pb(II). A regression equation was prepared using the coefficients which is as follows:

$$Y = 62.7674 - 10.0150 \times X_1 + 14.6917 \times X_2 + 2.5687 \times X_1^2 - 2.4763 \times X_2^2 - 0.6100 \times X_1 \times X_2 \quad (15)$$

where *Y* is the response variable, predicted % removal of Pb(II) adsorbed (mg/g). The low value of standard deviation (1.499) between the measured and predicted results shows that the equation adequately represents actual relationship between the response and significant variables. High values of R^2 (98.4%) and R^2 (adjusted) (97.3%) indicate a high dependence and correlation between the observed and the predicted values of response. This also indicates that 98.4% of result of the total variation can be explained by this model.

The statistical significance of the ratio of mean square variation due to regression and mean square residual error was tested using analysis of variance (ANOVA). ANOVA is a statistical technique that subdivides the total variation in a set of data into component parts

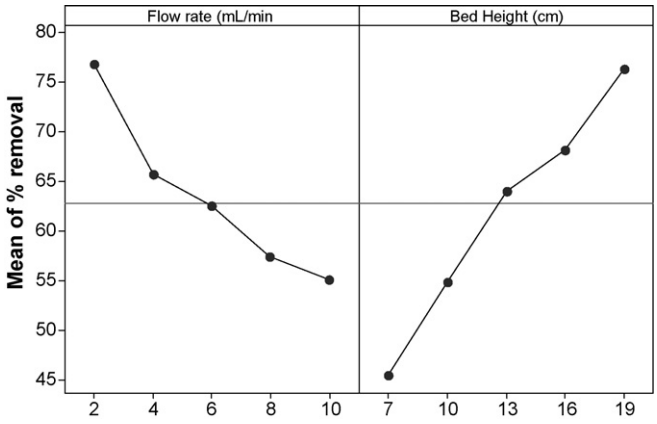

Fig. 5. Main effect plot.

associated with specific sources of variation for testing hypothesis on the parameters of the model [43]. According to Table 6b, the $F_{Statistics}$ values for all regression were higher (97.84). The large value of '*F*' indicates that most of the variation in the response can be explained by the regression equation. The associated *P*-value is used to estimate whether $F_{Statistics}$ is large enough to indicate statistical significance [44]. If *P*-value is lower than 0.05, it indicates that the model is statistically significant [45]. It was observed from ANOVA study that the coefficients for the linear ($P = 0.000$) and square terms ($P = 0.000$) were highly significant whereas interaction ($P = 0.834$) effect was not significant and thus the applicability of the predicted model is confirmed. The ANOVA table also shows no residual error which means the variation in the response data can be very well explained by the model.

3.6.2. Main effect plot

Main effect plots are drawn to compare the changes in the level means to see which factors influence the response the most. A main effect is present when different levels of a factor affect the response differently. It is created by plotting the response mean for each factor level. A line is drawn to connect the points for each factor and a reference line is also drawn at the overall mean. When the line is horizontal (parallel to the *x*-axis), there is no main effect present. Each level of the factor affects the response in the same way and the response mean is the same across all factor levels. When the line is not horizontal (parallel to the *x*-axis), there is a main effect present. Different levels of the factor affect the response differently. The greater the difference in the vertical position of the plotted points (the more the line is not parallel to the *x*-axis), the greater is the magnitude of the main effect [30,46].

The main effect of the parameter viz. flow rate and bed height on Pb(II) removal are given in Fig. 5 with reference line at 63.44. From the figures, it is observed that the flow rate has a negative effect on the removal of Pb(II). This figure also clears that the effect of bed height was positive on lead uptake. These plots show a clear

Table 6b
Analysis of variance (ANOVA) for the Pb(II) removal onto immobilized biomass of *A. hydrophila*.

Source	Degree of freedom	Seq SS	Adj SS	Adj MS	*F*-value	*P*-value
Regression	5	973.986	973.986	194.797	97.84	0.000
Linear	2	948.436	948.436	474.218	238.18	0.000
Square	2	25.457	25.457	12.729	6.39	0.022
Interaction	1	0.093	0.093	0.093	0.05	0.834
Residual Error	8	15.928	15.928	1.991		
Lack-of-Fit	3	15.928	15.928	5.309		
Pure Error	5	0.000	0.000	0.000		
Total	13	989.914				

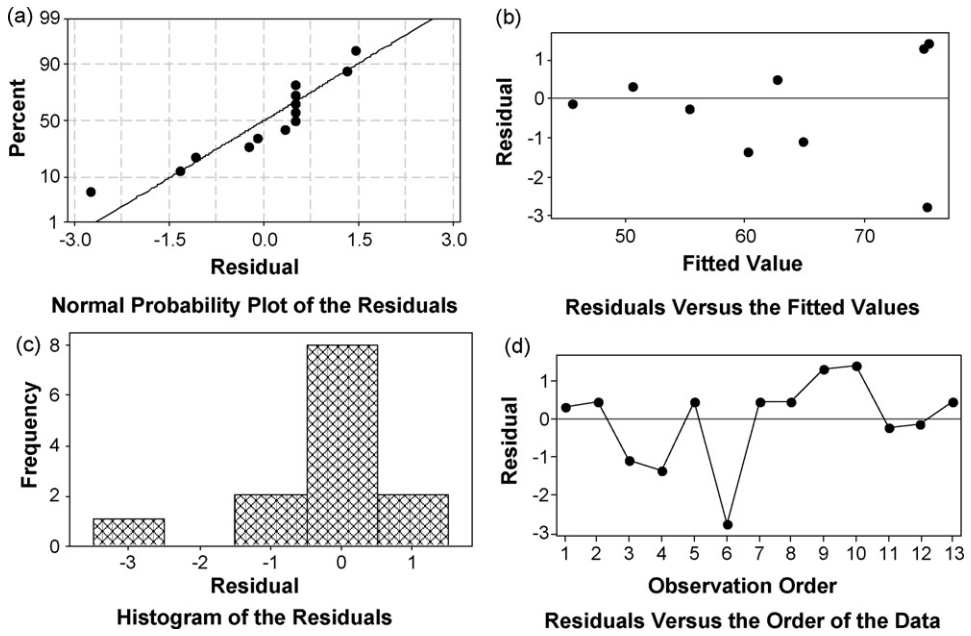

Fig. 6. Residual graphs (a) normal probability plot for residuals, (b) histograms of residuals, (c) residuals vs. fitted values and (d) residuals vs. the order of the data.

difference in the magnitude of the effect on the response among the factors flow rate and bed height indicating that the response % removal varies greatly with each of the factors studied.

3.6.3. Normal probability plot

The normality of the data can be checked by plotting the normal probability plot (NPP) of the residuals. The normal probability plot is a graphical technique for assessing whether or not a data set is approximately normally distributed [47]. The residual is the difference between the observed and the predicted value (or the fitted value) from the regression. If the points on the plot fall fairly close to the straight line, the data are normally distributed. Fig. 6(a) shows normal probability plot of residual values. It could be seen that the experimental points were reasonably aligned suggesting normal distribution. Fig. 6(b) plots the residuals vs. the fitted values (predicted response). The residuals are scattered randomly about zero i.e. the errors have a constant variance. The results can be shown in Fig. 6(c) with the help of a histogram. A histogram of the residuals shows the distribution of the residuals for all observations. The figure shows an almost symmetrical histogram (bell shaped, i.e. the errors are normally distributed with mean zero). This last plot of Fig. 6(d) is the residual value and the order of the corresponding observations. All the points were found to fall in the range of +3 to −3. No evidence of non-normality, skewness, outliers or unidentified variables exists. The plot is useful when the order of the observations may influence the results which can occur when data are collected in a line sequence. This plot can be helpful to a designed experiment in which the runs are not randomized. For lead % removal data, the residuals appear to be randomly scattered about zero. No evidence exists that the regression terms are correlated with one another.

3.6.4. Interpretation of contour plots

Contour plot is the projection of the response surface as a two-dimensional plane. This analysis gives a better understanding of the influence of variables and their interaction on the response. To investigate the interactive effect of two factors on the removal of lead, the response surface methodology was used and contour plots were drawn. The hold values of the remaining factors were set at their middle values (i.e. flow rate 6.0 mL/min and bed height 13 cm). Fig. 7 shows the combined effect of flow rate and bed height. The lines of contour plots predict the values of % lead removal for different bed height at different flow rate. These values are more or less same to the experimental values. The optimum 88.2760% Pb(II) removal was achieved at flow rate of 2.0 mL/min and bed height of 19.0 cm which is close to the experimental result i.e. 85.38% removal at same conditions.

3.6.5. Interpretation of process optimization curve

Response optimization helps to identify the factor settings that optimize a single response or a set of responses. It is useful in determining the operating conditions that will result in a desirable response. In the present study, the goal for % Pb(II) removal was to obtain a value at or near the target value of 90% removal. Percent removal less than 10 and greater than 100 was unacceptable.

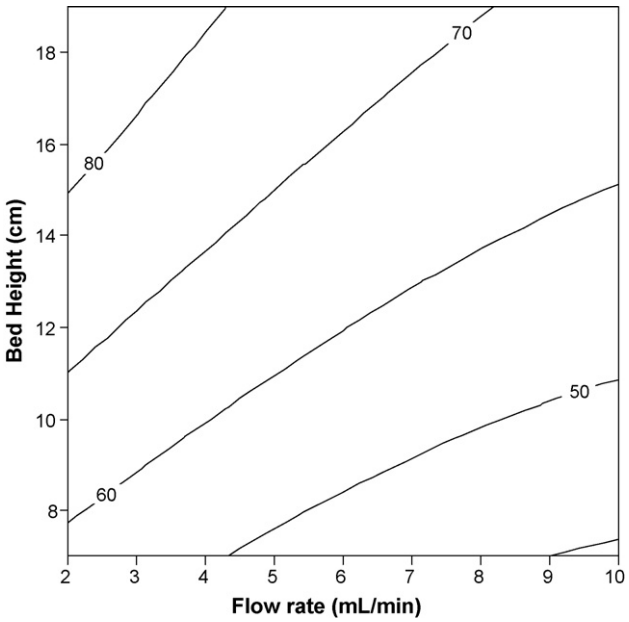

Fig. 7. Contour plot of Pb(II) biosorption.

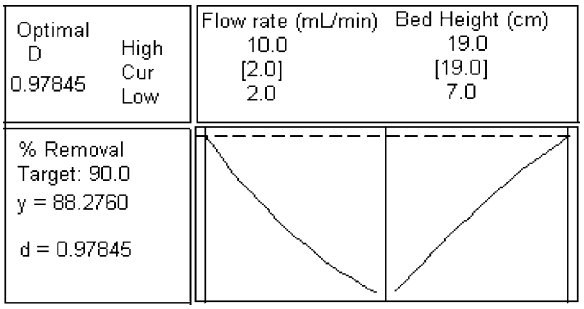

Fig. 8. Process optimization curve for a target value of 90% for Pb(II).

Both weight and importance were set at 1. The optimum condition i.e. the best combination of factor settings for achieving the optimum response was found to be flow rate 2.0 mL/min and bed height 19 cm for a predicted response of 88.2760% with a desirability score of 0.978 (Fig. 8). These results are found to be in good accordance with those obtained through experimentation. There are many advantages of optimization plot as it helps to achieve predicted response with higher desirability score, lower-cost factor settings with near optimal properties, to study the sensitivity of response variables to changes in the factor settings and to get required responses for factor settings of interest.

4. Conclusion

The following conclusions can be drawn from this study:

1. Free and immobilized biomass of *A. hydrophila* were successfully utilized for the removal of lead both in batch as well as in column system.
2. Langmuir isotherm model was found to fit to the sorption data indicating that sorption was monolayer and uptake capacity (Q^o) of biomass at pH 5.0 and 30 °C temperature were 163.9 and 138.88 mg/g for the free and immobilized biomass respectively.
3. A maximum of 85.38% Pb(II) removal from aqueous solution was achieved by breakthrough curve in up flow fixed bed column at bed height of 19 cm and flow rate of 2 mL/min at 103.6 mg/L Pb(II) concentration.
4. The Bed Depth Service Time model (BDST) was successfully utilized and in a good agreement with the experimental results ($r^2 > 0.997$).
5. Linear regression of the breakthrough time (t_b), uptake (Q) and critical bed length (Z_m) revealed that the sorption zone would reach top of the bed after 16 cycles, with the column bed completely getting exhausted after 33 cycles. The desorbent 0.01 M HCl provided uniform desorption efficiencies greater than 92.00% in all the three successive sorption–desorption cycles.
6. A 2^2 full factorial Central Composite Design was utilized with the help of MINITAB® Version15 Software for predicting the results with 14 sets of experiments and a high correlation has been found between the experimental and predicted results ($R^2 = 98.4\%$).
7. In this study, the data thus obtained would prove useful in designing an effluent treatment plant for Pb(II) rich effluents in batch as well as in column system.

Acknowledgments

The authors are thankful to Institute of Technology, Banaras Hindu University and University Grant Commission (UGC) (F.No. 32-224/2006 (SR)) for laboratory facilities and financial assistance.

References

[1] B. Volesky, Z.R. Holan, Biosorption of heavy metals, Biotechnol. Prog. 11 (1995) 235–250.
[2] S.H. Hasan, P. Srivastava, M. Talat, Biosorption of Pb(II) from water using biomass of *Aeromonas hydrophila*: central composite design for optimization of process variables, J. Hazard. Mater. 168 (2009) 1155–1162.
[3] A.K. De, Environmental Chemistry, New age publisher International Publication, New York, 2000.
[4] N. Ahalya, T.V. Ramachandra, R.D. Kanamadi, Biosorption of heavy metals, J. Chem. Environ 7 (2003) 71–79.
[5] D. Ranjan, P. Srivastava, M. Talat, S.H. Hasan, Biosorption of Cr(VI) from water using biomass of *Aeromonas hydrophila*: Central Composite Design for optimization of process variables, Appl. Biochem. Biotechnol. 158 (2009) 524–539.
[6] R.H.S.F. Viera, B. Volesky, Biosorption: a solution to pollution? Int. Microbiol. 3 (2000) 17–24.
[7] K. Vijayaraghavan, Y.S. Yun, Bacterial biosorbents and biosorption, Biotechnol. Adv. 26 (2008) 266–291.
[8] D. Sud, G. Mahajan, M.P. Kaur, Agricultural waste material as potential adsorbent for sequestering heavy metal ions from aqueous solutions—a review, Bioresour. Technol. 99 (2008) 6017–6027.
[9] S.S. Ahluwalia, D. Goyal, Microbial and plant derived biomass for removal of heavy metals from wastewater, Bioresour. Technol. 98 (2007) 2243–2257.
[10] N.V. Medvidović, J. Perić, M. Trgo, M.N. Mužek, Removal of lead ions by fixed bed of clinoptilolite—the effect of flow rate, Micropor. Mesopor. Mater. 105 (2007) 298–304.
[11] R. Han, J. Zhang, W. Zou, H. Xiao, J. Shi, H. Liu, Biosorption of copper(II) and lead(II) from aqueous solution by chaff in a fixed-bed column, J. Hazard. Mater. B133 (2006) 262–268.
[12] K.C. Sekhar, C.T. Kamala, N.S. Chary, A.R.K. Sastry, T. Nageswara Rao, M. Vairamani, Removal of lead from aqueous solutions using an immobilized biomaterial derived from a plant biomass, J. Hazard. Mater. B108 (2004) 111–117.
[13] K. Vijayaraghavan, Y.S. Yun, Polysulfone-immobilized *Corynebacterium glutamicum*: a biosorbent for reactive black 5 from aqueous solution in an up-flow packed column, Chem. Eng. J. 145 (2008) 44–49.
[14] Z. Aksu, F. Gönen, Biosorption of phenol by immobilized activated sludge in a continuous packed bed: prediction of breakthrough curves, Process. Biochem. 39 (2004) 599–613.
[15] J.H. Hunik, J. Trumper, Large-scale production of κ-carrageenan droplets for gels beads production: theoretical and practical limitations of size and production rate, Biotechnol. Progr. 9 (1993) 186–192.
[16] D. Rome, G.L. Gadd, Use of pelleted and immobilized yeast and fungal biomass for heavy metals and radionuclide recovery, J. Ind. Microbiol. (1991) 97–104.
[17] O. Smidsr d, G. Skjak-Barek, Alginate as immobilization matrix of cells, Trends Biotechnol. 7 (1990) 71–78.
[18] D.P. Mungasavalli, T. Viraraghavan, Y.C. Jin, Biosorption of chromium from aqueous solutions by pretreated *Aspergillus niger*: batch and column studies, Colloids Surf. A 301 (2007) 214–223.
[19] G. Yan, T. Viraraghavan, M. Chen, A new model for heavy metal removal in a biosorption column, Adsorpt. Sci. Technol. 19 (2001) 25–43.
[20] S.H. Hasan, P. Srivastava, D. Ranjan, M. Talat, Biosorption of Cr(VI) from aqueous solution using *A. hydrophila* in up-flow column: optimization of process variables, Appl. Microbiol. Biotechnol. 83 (2009) 567–577.
[21] A.I. Khuri, S.A. Cornell, Response Surface Design and Analysis of Experiment, Marcel Dekker Inc., New York, 1987.
[22] R.I. Mason, R.F. Funst, J.L. Hess, Statistical Design and Analysis of Experiments, Wiley, New York, 1989.
[23] F.J. Heck, S.H. Floris, P.F. Herty, M.A.Z. Ayub, Optimization of cellulose-free xylanose activity produced by *Bacillus coagulans* BL69 in solid-state cultivation, Process. Biochem. 40 (2005) 107–112.
[24] I.D. Mall, V.C. Srivastava, G.V.A. Kumar, I.M. Mishra, Characterization and utilization of mesoporous fertilizer plant waste carbon for adsorptive removal of dyes from aqueous solution, Colloids Surf. A 278 (2006) 175–187.
[25] L.S. Balistrieri, J.W. Murray, The surface chemistry of goethite (α-FeOOH) in major sea water, Am. J. Sci. 281 (1981) 788–806.
[26] Vogel's Text Book of quantitative Chemical analysis, 5th edition, Bath Press Ltd., UK.
[27] K. Vijayaraghvan, J. Palanivelu, M. Velan, Removal of nickel(II) ions from aqueous solution using Crab shells particles in a packed bed up-flow column, J. Hazard. Mater. B 113 (2004) 223–230.
[28] R.A. Hutchins, New method simplifies design of activated carbon systems, Am. J. Chem. Eng. 80 (1973) 133–138.
[29] M.Y. Can, Y. Kaya, O.F. Algur, Response surface optimization of the removal of nickel from aqueous solution by cone biomass of *Pinus sylvestris*, Bioresour. Technol. 97 (2006) 1761–1765.
[30] K. Ravikumar, S. Krishnan, S. Ramalingam, K. Balu, Application of response surface methodology to optimize the process variable for reactive Red and Acid Brown dye removal using a novel adsorbent, Dyes Pigments 72 (2007) 66–74.
[31] A. Kumar, B. Prasad, I.M. Mishra, Optimization of process parameter for acrylonitrile removal by low cost adsorbent using Box-Behnken design, J. Hazard. Mater. 150 (2008) 174–182.
[32] MINITAB® Release 15 Statistical Software for Windows, Minitab Inc., USA, 2006.
[33] V.J.P. Vilar, C.M.S. Botelho, R.A.R. Boaventure, Influence of pH, ionic strength and temperature on lead biosorption by Gelidium and agar extraction algal waste, Process. Biochem. 40 (2005) 3267–3275.

[34] N. Kuyucak, B. Volesky, The mechanism of cobalt biosorption, Biotechnol. Bioeng. 339 (1989) 823–831.
[35] A. Singh, D. Kumar, J.P. Gaur, Copper(II) and lead(II) sorption from aqueous solution by non-living *Spirogyra neglecta*, Bioresour. Technol. 98 (2007) 3622–3629.
[36] I. Langmuir, The adsorption of gases on plane surfaces of glass, mica and platinum, J. Am. Chem. Soc. 40 (1918) 1361–1403.
[37] R.S. Bai, T.E. Abraham, Studies on Cr(VI) adsorption–desorption using immobilized fungal biomass, Bioresour. Technol. 87 (2003) 17–26.
[38] P. Lodeiro, R. Herrero, M.E. Sastre de Vicente, The use of protonated *Sargassum muticum* as biosorbent for cadmium removal in a fixed-bed column, J. Hazard. Mater. B137 (2006) 244–253.
[39] Z. Zulfadhly, M.D. Mashitah, S. Bhatia, Heavy metals removal in fixed bed column by the macro fungus *Pycnoporus sanguineus*, Environ. Pollut. 112 (2001) 463–470.
[40] V.C. Taty-Costodes, H. Fauduet, C. Porte, Y.S. Ho, Removal of Pb(II) ions from synthetic and real effluents using immobilized *Pinus sylvestris* saw dust: adsorption on a fixed bed column, J. Hazard. Mater. 123 (B) (2005) 135–144.
[41] K. Vijayaraghvan, D. Prabhu, Potential of *Sargassum wightii* biomass for copper (II) removal from aqueous solutions: application of different mathematical models to batch and continuous biosorption data, J. Hazard. Mater. B137 (2006) 558–564.
[42] B. Volesky, J. Weber, J.M. Park, Continuous-flow metal biosorption in a regenerable Sargassum column, Water Res. 37 (2003) 297–306.
[43] J. Segurola, N.S. Allen, M. Edge, A.M. Mahon, Design of eutectic photo initiator blends for UV/curable curable acrylated printing inks and coatings, Prog. Org. Coat. 37 (1999) 23–37.
[44] H.M. Kim, J.G. Kim, J.D. Cho, J.W. Hong, Optimization and characterization of U.V.-curable adhesives for optical communication by response surface methodology, Polym Test 22 (2003) 899–906.
[45] M.M.D. Zulkali, A.L. Ahmad, N.H. Norulakmal, *Oryza sativa* L. husk as heavy metal adsorbent: optimization with lead as model solution, Bioresour. Technol. 97 (2006) 21–25.
[46] D. Pokhrel, T. Viraraghvan, Arsenic removal from aqueous solution by iron oxide coated fungal biomass: a factorial design analysis, Water Air Soil Pollut. 173 (2006) 195–208.
[47] G.E.P. Box, J.S. Hunter, Multifactor experimental design for exploring response surfaces, Ann. Math. Stat. 28 (1957) 195–241.